A Journal of the Gesellschaft Deutscher Chemiker
Angewandte Chemie
GDCh
International Edition
www.angewandte.org

Accepted Article

Title: Helix to Super-Helix Transition in π-Systems Self-assembly: Superseding of Molecular Chirality at Hierarchical Level

Authors: Mohamed Hifsudheen, Rakesh K Mishra, Balaraman Vedhanarayanan, Vakayil K Praveen, and Ayyappanpillai Ajayaghosh

To be cited as: *Angew. Chem. Int. Ed.* 10.1002/anie.201707392
Angew. Chem. 10.1002/ange.201707392

Link to VoR: http://dx.doi.org/10.1002/anie.201707392
http://dx.doi.org/10.1002/ange.201707392

WILEY-VCH

Helix to Super-Helix Transition in π-Systems Self-assembly: Superseding of Molecular Chirality at Hierarchical Level

*Mohamed Hifsudheen, Rakesh K. Mishra, Balaraman Vedhanarayanan, Vakayil K. Praveen,** and *Ayyapanpillai Ajayaghosh**

Abstract: *Higher-order super-helical structures derived from biological molecules are known to evolve through opposite coiling of the initial helical fibers as seen in the case of collagen protein. Herein we describe a similar kind of phenomenon in a π-system self-assembly of chiral oligo(phenyleneethylene) derivatives (S)-**1** and (R)-**1** which explains the unequal formation of both left- and right-handed helices from molecule having a specific chiral center. The concentration and temperature-dependent circular dichroism (CD) and UV-Vis spectroscopic studies revealed that the initial formation of helical aggregates is in accordance with the molecular chirality. However, at the next level of hierarchical self-assembly, coiling of the fibers occurs with opposite handedness, thereby superseding the command of the molecular chirality. This has been confirmed with the help of solvent-dependent decoiling of super-helical structures and concentration-dependent morphological analysis. While this phenomenon is common in biological system, this is the first time to have detailed mechanistic insight for synthetic molecules, which explains the occurrence of both left- and right-handed helical assemblies from the same chiral molecule.*

Helical architectures constitute one of the most aesthetic and unique systems evolved during the origin of life on earth. DNA and proteins are some of the well-known examples of helical biopolymers. These biopolymers often undergo transition from lower-order structures to higher-order super-helical structures to achieve more precision, selectivity and efficiency in their functions.[1] For instance, coiled-coil super-helical structures of proteins such as collagen are responsible for providing high strength to cartilage and bone. On the other hand, in some other cases formation of higher-order helical structures are responsible for several neurodegenerative disorders.[1b] It is interesting to note that in most of the cases the final helicity of the super structures are not in agreement with the chirality of molecular building blocks involved. Therefore, mechanistic insights on their formation are of paramount importance.

To mimic the complex biological functions involving helical structures, chemists have been trying to replicate these processes functionally and morphologically by developing synthetic helical systems.[2-6] Transfer of chirality can takes place from (i) single molecules to one-dimensional (1D) assemblies and then from (ii) 1D helical assemblies to macroscopic superstructures. In principle, each step in this propagation process can determine the overall supramolecular chirality of the system and therefore, sometimes creates ambiguity in predicting the handedness of helical assemblies. Recently, Meijer and co-workers have demonstrated that pathway complexity in the nucleation-elongation process can determine the helical handedness of 1D assemblies formed from a synthetic π-system.[7] While the role of hierarchical processes like helix to super-helix transformation in defining the supramolecular chirality of assemblies formed by biopolymers is well established,[5a,c] this aspect has been overlooked in the case of synthetic supramolecular polymers.[5d,8] Herein, we report a mechanistic insight into the transformation of the initial 1D helical structures to super-helical fibers with opposite handedness. In this hierarchical assembly process, the overall chirality supersedes the molecular chirality, resulting in oppositely coiled helical bundles, which can be systematically decoiled under appropriate experimental conditions.

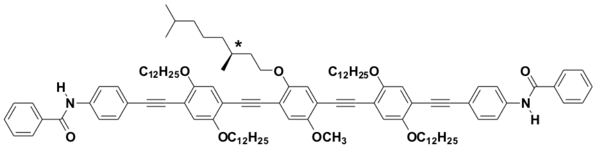

(S)-1

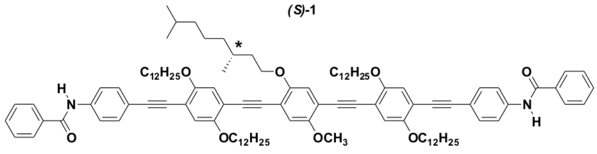

(R)-1

We have chosen the amide functionalized phenyleneethynylene (PE) derivatives *(S)*-**1** and *(R)*-**1** having a single chiral handle[9] at the center of the molecule. *(S)*-**1** and *(R)*-**1** were synthesized by multistep palladium-catalyzed Sonogashira–Hagihara cross coupling reactions (Scheme S1) and characterized by FT-IR, ^{1}H and ^{13}C NMR spectroscopy as well as by high-resolution mass spectrometry (Figure S1-S3). At a concentration of 5×10^{-6} M, the UV-Vis absorption spectra of *(S)*-**1** and *(R)*-**1** in chloroform at 280 K showed a broad π-π* absorption band at 404 nm (Figure S4a), whereas in *n*-decane, the absorption spectrum was more structured with the appearance of an additional band at 460 nm (Figure S4a). Upon increasing the temperature from 280 to 330 K, the absorption spectrum in *n*-decane lost its features and became broad similar to that in chloroform (Figure S4b) implying that at 280 K, both *(S)*-**1** and *(R)*-**1** form aggregates in *n*-decane, whereas in chloroform they are dissolved.

M. Hifsudheen, Dr. R. K. Mishra, Dr. B. Vedhanarayanan,
Dr. V.K. Praveen, Prof. Dr. A. Ajayaghosh
Photosciences and Photonics Section, Chemical Science and Technology Division
CSIR-National Institute for Interdisciplinary Science and Technology (CSIR-NIIST), Thiruvananthapuram 695019 (India)
E-mail: ajayaghosh@niist.res.in
vkpraveen@niist.res.in

M. Hifsudheen, Dr. B. Vedhanarayanan, Dr. V.K. Praveen,
Prof. Dr. A. Ajayaghosh
Academy of Scientific and Innovative Research (AcSIR)
CSIR-NIIST Campus, Thiruvananthapuram 695019 (India)

Supporting information for this article is given via a link at the end of the document

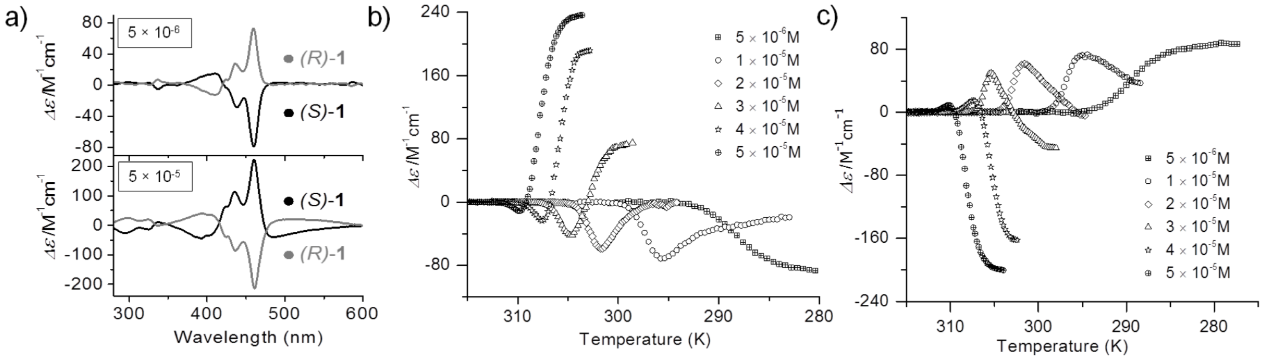

Figure 1. a) CD Spectra of *(S)*-**1** (black) and *(R)*-**1** (gray) at concentrations of 5 × 10^{-6} M (upper panel) and 5 × 10^{-5} M (lower panel) in *n*-decane. b) CD spectral intensity variations of *(S)*-**1** and c) *(R)*-**1** measured at λ = 460 nm upon cooling (1 K min^{-1}) of *n*-decane solutions at different concentrations.

Aggregates of both *(S)*-$\mathbf{1}_{\mathbf{agg}}$ and *(R)*-$\mathbf{1}_{\mathbf{agg}}$ prepared by heating and controlled cooling (1 K min^{-1}) exhibited mirror image CD spectra with opposite Cotton effects (Figure 1a and S5). For example, at 280 K, CD spectrum of *(S)*-$\mathbf{1}_{\mathbf{agg}}$ (5×10^{-6} M) showed a bisignate Cotton effect with a negative signal at 460 nm followed by a positive signal at 410 nm with a zero crossing at 419 nm. On the contrary, *(R)*-$\mathbf{1}_{\mathbf{agg}}$ (5×10^{-6} M) exhibited a positive signal at 460 nm followed by a negative signal at 410 nm (Figure 1a upper panel). Surprisingly, the CD spectra recorded at a higher concentration of 5 × 10^{-5} M displayed a complete reversal in the chiral signature of both *(S)*-$\mathbf{1}_{\mathbf{agg}}$ and *(R)*-$\mathbf{1}_{\mathbf{agg}}$ with 3-fold enhancement in CD spectral intensity (Figure 1a lower panel). The observed chirality reversal at higher concentration was studied by temperature dependent (cooling rate 1 K min^{-1}) CD spectral intensity variation of *(S)*-$\mathbf{1}_{\mathbf{agg}}$ at λ = 460 nm. Cooling curves obtained at different concentrations of *(S)*-**1** showed an independent nature (Figure 1b). At a lower concentration of 5 × 10^{-6} M, CD cooling curve shows a complete negative signal, while upon increasing concentration up to 2 × 10^{-5} M, cooling curves initially showed a negative trend, however, revert back to zero. Above this critical concentration, the CD intensity for all the cooling curves reaches to a positive value, after passing through a negative dip. The corresponding CD spectra also exhibited a gradual change in Cotton effect from negative to positive upon increasing concentration (Figure S6a). Exactly opposite trends were observed for CD spectra and cooling curves for *(R)*-**1** (Figure 1c and S6b).

To probe the self-assembly pathway of *(S)*-**1** in *n*-decane, the UV-Vis absorption changes at 460 nm were monitored as a function of temperature by fixing the cooling rate 1 K min^{-1}. The plot of degree of aggregation (α_{agg}) against temperature reveals non-sigmoidal nature of cooling curves (Figure S7). The cooling curves can be fitted with a nucleation-elongation model characteristic of a cooperative assembly[10] and the data are summarized in Table S1. The curve fitting provided the elongation enthalpy, ΔH_{e} = −128.1 kJ mol^{-1}, elongation temperature, T_{e} = 294.1 K and degree of cooperativity, K_{a} = 2.2 x 10^{-5} at a given concentration of 5 x 10^{-6} M. Upon increasing the concentration to 5 x 10^{-5} M, significant changes are observed in ΔH_{e} (−258.8 kJ mol^{-1}), T_{e} (312.1 K) and K_{a} (1.1 x 10^{-5}). This observation implies that *(S)*-**1** self-assembles through an enthalpically driven cooperative process involving multiple noncovalent interactions such as π-π stacking and H-bonding (Figure S8). The concentration dependent increase in T_{e} shows a linear relationship in the van't Hoff plot (Figure S9) yielding the standard enthalpy ($\Delta H°$) and entropy ($\Delta S°$) values of -101.7 kJ mol^{-1} and 244.4 J mol^{-1} K^{-1}, respectively. At lower concentrations ΔH_{e} values show close agreement with $\Delta H°$, while at higher concentrations a significant deviation is noticed. The increased negative enthalpy release observed at higher concentrations suggests clustering[5a,10a] and coiling of helical aggregates to super-helical structures,[5a,5d,8] which can be correlated to inversion of CD signal with increase in intensity at higher concentrations. Temperature-dependent heating of (1 K min^{-1}) aggregates in *n*-decane exhibited decrease in the CD spectral intensity of *(S)*-$\mathbf{1}_{\mathbf{agg}}$ at λ = 460 nm from the initial positive to negative value followed by a gradual increase to zero. The presence of aggregates having negative CD signal in the temperature-dependent heating and cooling experiments (Figure

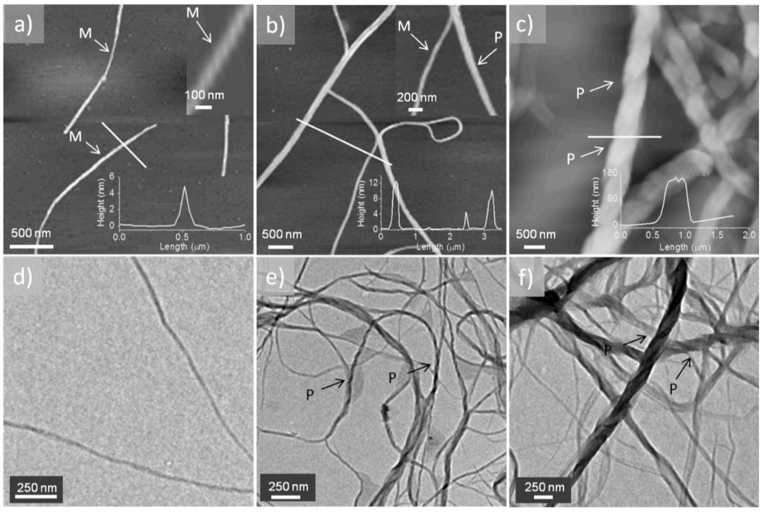

Figure 2. AFM with height profiles and TEM images of *(S)*-$\mathbf{1}_{\mathbf{agg}}$ in *n*-decane at a concentration of a) and d) 5 × 10^{-6} M, b) and e) 2 × 10^{-5} M and c) and f) 5 × 10^{-5} M, respectively. The insets of a and b show zoomed images. Helicity of the fibers are indicated with arrows.

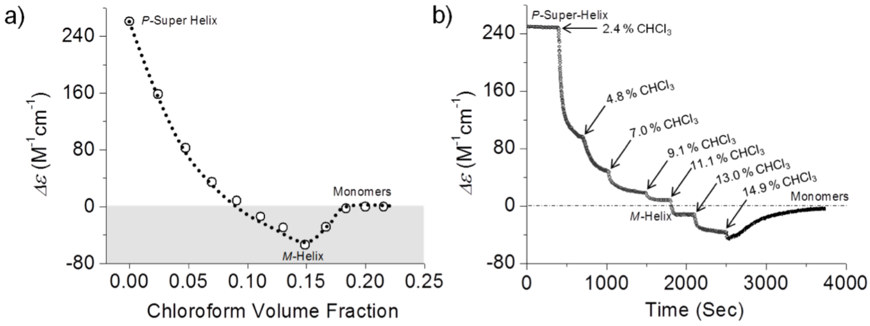

Figure 3. a) Decoiling of *(S)*-$\mathbf{1}_{\mathbf{Agg}}$ (5 × 10^{-5} M) in *n*-decane induced by manually mixing different volume fractions of *(S)*-**1** in chloroform (5 × 10^{-5} M) while keeping the total concentration of the mixture as 5 × 10^{-5} M. b) Decoiling kinetics of *(S)*-$\mathbf{1}_{\mathbf{agg}}$ (5 × 10^{-5} M) in *n*-decane studied by injecting different volume fractions of *(S)*-**1** in chloroform (5 × 10^{-5} M).

S10 and S11) indicate that the formation of helical aggregates at higher concentration follow a thermodynamic pathway and rules out the existence of off-pathway or metastable aggregates.[7,11]

AFM images of *(S)*-$\mathbf{1}_{\mathbf{agg}}$ prepared at lower concentration (5×10^{-6} M) showed the formation of left-handed (*M*-type) helical fibers of width ranging from 100-150 nm with helical pitch of 70-80 nm (Figure 2a). The heights of these fibers were in the range of 4-6 nm. At 2 x 10^{-5} M, coiling of fibers is observed (Figure 2b and S12a) and at 5×10^{-5} M densely coiled helical bundles of width 500-700 nm and height of 150-170 nm could be seen (Figure 2c and S12b). The helicity of these super-helical fibers were found to be right-handed (*P*-type) along with a few *M*-type helical fibers. The TEM images recorded at lower (Figure 2d, 2e and S13a) and higher concentrations (Figure 2f and S13b) of *(S)*-**1** also indicate the coiling of individual 1D helical fibers to super helical fiber bundles of opposite handedness. In the TEM image, even though we could not clearly see the initial helicity of fibers, the final helicity of the supercoils is clear, which is in agreement with the AFM image.

To rationalize the formation of super-helix with opposite handedness, a solvent assisted[12,13] decoiling study of *(S)*-$\mathbf{1}_{\mathbf{agg}}$ was performed. Careful addition of a solution of *(S)*-**1** in chloroform (5 x 10^{-5} M) to a solution of *(S)*-$\mathbf{1}_{\mathbf{agg}}$ in *n*-decane (5 x 10^{-5} M) at different ratios resulted in changes in CD spectral intensity at λ = 460 nm, which was plotted against chloroform volume fraction (v/v), *f* (Figure 3a and S14). Even at a very small volume fraction (*f* = 0.024), a substantial decrease in CD intensity was observed. As the chloroform ratio was increased, the changes in CD intensity became negative at a volume fraction of *f* = 0.111, and showed maximum negative dip at *f* = 0.149. Upon further increase in the chloroform fraction (*f* = 0.183), complete disappearance of CD signal was observed. These observations confirm the decoiling of the *P*-super helix to the 1D *M*-fibers and the subsequent depolymerization to the respective monomer. This has been again confirmed by probing the time-dependent variation in CD intensity at λ = 460 nm after injecting different fractions of molecularly dissolved *(S)*-**1** in chloroform (5 x 10^{-5} M) to a solution of (*S*)-$\mathbf{1}_{\mathbf{agg}}$ in *n*-decane (5 x 10^{-5} M) at different time scale (Figure 3b).

Dilution of (*S*)-$\mathbf{1}_{\mathbf{agg}}$ or (*R*)-$\mathbf{1}_{\mathbf{agg}}$ (5 x 10^{-5} M) in *n*-decane with the same solvent did not show any change in CD response when $\Delta\varepsilon$ is plotted against concentration (Figure 4a). This observation indicates that the super-helical fibers once formed in *n*-decane are quite stable and is resistant to decoiling or disassembly upon dilution with a nonpolar solvent. The effect of temperature on the CD intensity variation of *M*-helix of *(S)*-$\mathbf{1}_{\mathbf{agg}}$ (5 x 10^{-6} M) and *P*-super-helix (5 × 10^{-6} M) prepared by dilution of *(S)*-$\mathbf{1}_{\mathbf{agg}}$ (5 x 10^{-5} M) is shown in Figure 4b. Heating the *M*-helix of *(S)*-$\mathbf{1}_{\mathbf{agg}}$ (5 x 10^{-6} M) leads to depolymerization to monomers (Figure 4b, pink), whereas heating the *P*-super helix of *(S)*-$\mathbf{1}_{\mathbf{agg}}$ (5 × 10^{-6} M) leads to decoiling followed by depolymerization to monomers (Figure 4b, blue). Based on the above observation, the chiral self-assembly of *(S)*-$\mathbf{1}_{\mathbf{agg}}$ or (*R*)-$\mathbf{1}_{\mathbf{agg}}$ can be explained as shown in Figure 5. Initially, the molecules form 1D helical fibers in agreement with the molecular chirality, following a nucleation-elongation pathway. At higher concentration, the 1D helical fibers coil to form super-helical fiber bundles with opposite handedness. These super helices undergo decoiling upon adding polar solvents as a denaturant or increasing the temperature.

In summary, insights on the complex pathway associated with helical to super-helical transformation of a synthetic π-system assembly, which follows a nucleation-elongation mechanism is disclosed. The helical to super-helical transformation observed in the present system is reminiscent of the super-helix formation of biopolymers such as proteins. This

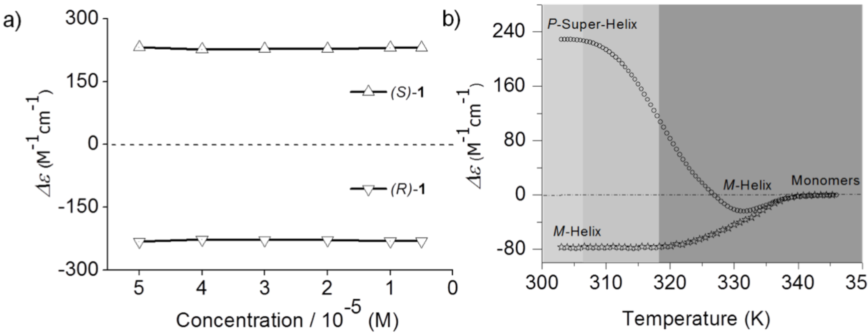

Figure 4. a) The plot of CD intensity in $\Delta\varepsilon$ (λ = 460 nm) versus concentration. The data is obtained from the dilution experiment conducted by adding *n*-decane to a solution of *(S)*-$\mathbf{1}_{\mathbf{Agg}}$ and *(R)*-$\mathbf{1}_{\mathbf{Agg}}$ in *n*-decane (5 x 10^{-5} M) prepared by controlled cooling (1 K min^{-1}). b) Change in CD spectral intensity at λ = 460 nm upon heating *M*-helix of *(S)*-$\mathbf{1}_{\mathbf{Agg}}$ (5 × 10^{-6} M) in *n*-decane prepared by controlled cooling (○) and *P*-super-helix of *(S)*-**1** (5 × 10^{-6} M) (☆) prepared by diluting *(S)*-$\mathbf{1}_{\mathbf{Agg}}$ (5 × 10^{-5} M) in *n*-decane with the same solvent.

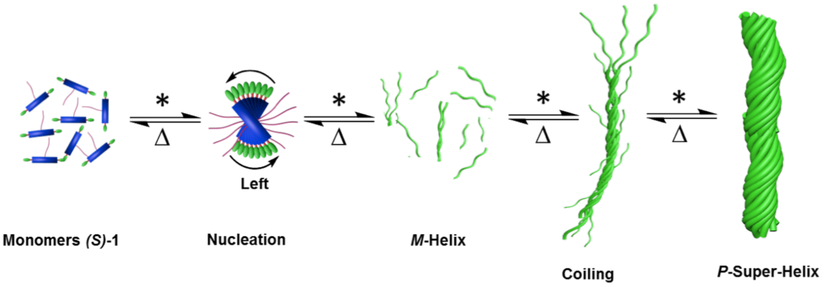

Figure 5. Schematic representation of the nucleation-elongation self-assembly pathway leading to super-helical formation on (*S*)-**1** in *n*-decane.

study explains the ambiguity existing in several of the previous reports on the formation of different amounts of left- and right-handed assemblies from a molecule having one specific chiral handle.

Acknowledgements

A.A. is grateful to the DST-SERB, Govt. of India, for a J. C. Bose National Fellowship (SB/S2/JCB-11/2014). M.H. and B.V. are thankful to CSIR, Govt. of India, for research fellowships. R.K.M. acknowledges, DST for an Inspire Faculty Fellowship. V.K.P. thanks DST-SERB, for a Young Scientist Fellowship. We thank Mr. Kiran Mohan and Dr. R. Panneerselvam (CSIR-NIIST) for TEM and data fitting, respectively.

Keywords: π-system • self-assembly • chirality • super-helix • CD-inversion

[1] a) J. Adamcik, J.-M. Jung, J. Flakowski, P. De Los Rios, G. Dietler, R. Mezzenga, *Nature Nanotech* **2010**, *5*, 423–428; b) A. Aguzzi, T. O'Connor, *Nat. Rev. Drug Discov.* **2010**, *9*, 237–248.

[2] a) A. R. A. Palmans, E. W. Meijer, *Angew. Chem. Int. Ed.* **2007**, *46*, 8948–8968; *Angew. Chem.* **2007**, *119*, 9106–9126; b) L. Pérez-García, D. B. Amabilino, *Chem. Soc. Rev.* **2007**, *36*, 941–967; c) V. K. Praveen, S. S. Babu, C. Vijayakumar, R. Varghese, A. Ajayaghosh, *Bull. Chem. Soc. Jpn.* **2008**, *81*, 1196–1211; d) S. S. Babu, V. K. Praveen, A. Ajayaghosh, *Chem. Rev.* **2014**, 114, 1973–2129; e) M. Liu, L. Zhang, T. Wang, *Chem. Rev.* **2015**, 115, 7304-7397; f) E. Yashima, N. Ousaka, D. Taura, K. Shimomura, T. Ikai, K. Maeda, *Chem. Rev.* **2016**, *116*, 13752–13990; g) D. B. Amabilino, D. K. Smith, J. W. Steed, *Chem. Soc. Rev.* **2017**, *46*, 2404–2420.

[3] a) A. Lohr, M. Lysetska, F. Würthner, *Angew. Chem. Int. Ed.* **2005**, 44, 5071–5074; *Angew. Chem.* **2005**, *117*, 5199–5202; b) W. Zhang, W. Jin, T. Fukushima, N. Ishii, T. Aida, *J. Am. Chem. Soc.* **2013**, *135*, 114–117; c) X. Ma, Y. Zhang, Y. Zhang, Y. Liu, Y. Che, J. Zhao, *Angew. Chem. Int. Ed.* **2016**, *55*, 9539–9543; *Angew. Chem.* **2016**, *128*, 9691–9695; d) S. Dhiman, A. Jain, S. J. George, *Angew. Chem. Int. Ed.* **2017**, *56*, 1329–1333; *Angew. Chem.* **2017**, *129*, 1349–1353; e) T. Goto, Y. Okazaki, M. Ueki, Y. Kuwahara, M. Takafuji, R. Oda, H. Ihara, *Angew. Chem. Int. Ed.* **2017**, *129*, 3035–3039; *Angew. Chem.* **2017**, *129*, 3035–3039.

[4] a) F. Aparicio, B. Nieto-Ortega, F. Najera, F. J. Ramírez, J. T. López Navarrete, J. Casado, L. Sánchez, *Angew. Chem. Int. Ed.* **2014**, *53*, 1373–1377; *Angew. Chem.* **2014**, *126*, 1397–1401; b) L. Đorđević, T. Marangoni, T. Miletić, J. Rubio-Magnieto, J. Mohanraj, H. Amenitsch, D. Pasini, N. Liaros, S. Couris, N. Armaroli, M. Surin, D. Bonifazi, *J. Am. Chem. Soc.* **2015**, *137*, 8150–8160; c) J. Labuta, J. P. Hill, S. Ishihara, L. Hanyková, K. Ariga, *Acc. Chem. Res.* **2015**, *48*, 521–529; d) Y. Kim, H. Li, Y. He, X. Chen, X. Ma, M. Lee, *Nat. Nanotech.* **2017**, *12*, 551–556; e) D. Yang, L. Zhang, P. Duan, M. Liu, *Nat. Commun.* **2017**, *8*, 15727.

[5] a) A. Aggeli, I. A. Nyrkova, M. Bell, R. Harding, L. Carrick, T. C. B. McLeish, A. N. Semenov, N. Boden, *Proc. Natl. Acad. Sci.* **2001**, *98*, 11857–11862; b) M. A. J. Gillissen, M. M. E. Koenigs, J. J. H. Spiering, Jef A. J. M. Vekemans, A. R. A. Palmans, I. K. Voets, and E. W. Meijer, *J. Am. Chem. Soc.* **2014**, *136*, 336–343; c) S. Mondal, L. Adler-Abramovich, A. Lampel, Y. Bram, S. Lipstman, E. Gazit, *Nat. Commun.* **2015**, *6*, 8615; d) M. Yamauchi, T. Ohba, T. Karatsu, S. Yagai, *Nat. Commun.* **2015**, 6, 8936.

[6] a) S. J. George, A. Ajayaghosh, P. Jonkheijm, A. P. H. J. Schenning, E. W. Meijer, *Angew. Chem. Int. Ed.* **2004**, *43*, 3422–3425; *Angew. Chem.* **2004**, *116*, 3504–3507; b) A. Ajayaghosh, C. Vijayakumar, R. Varghese, S. J. George, *Angew. Chem. Int. Ed.* **2006**, *45*, 456–460; *Angew. Chem.* **2006**, *118*, 470–474; c) A. Ajayaghosh, R. Varghese, S. Mahesh, V. K. Praveen, *Angew. Chem. Int. Ed.* **2006**, *45*, 7729–7732; *Angew. Chem.* **2006**, *118*, 7893–7896; d) A. Gopal, M. Hifsudheen, S. Furumi, M. Takeuchi, A. Ajayaghosh, *Angew. Chem. Int. Ed.* **2012**, *51*, 10505-10509; *Angew. Chem.* **2012**, *124*, 10657–10661; e) B. Vedhanarayanan, V. S. Nair, V. C. Nair, A. Ajayaghosh, *Angew. Chem. Int. Ed.* **2016**, *55*, 10345–10349; *Angew. Chem.* **2016**, *128*, 10501–10505.

[7] P. A. Korevaar, S. J. George, A. J. Markvoort, M. M. Smulders, P. A. Hilbers, A. P. H. J Schenning, T. F. De Greef, E. W. Meijer, *Nature* **2012**, 481, 492–496.

[8] For morphological evidence of super-helical structure formation, see: a) H. Engelkamp, S. Middelbeek, R. J. M. Nolte, *Science* **1999**, *284*, 785−788; b) O.-K. Kim, J. Je, G. Jernigan, L. Buckley, D. Whitten, *J. Am. Chem. Soc.* **2006**, *128*, 510–516; c) I. Danila, F. Riobé, F. Piron, J. Puigmartí-Luis, J. D. Wallis, M. Linares, H. Ågren, D. Beljonne, D. B. Amabilino, N. Avarvari, *J. Am. Chem. Soc.* **2011**, *133*, 8344–8353.

[9] a) P. Iavicoli, H. Xu, L. N. Feldborg, M. Linares, M. Paradinas, S. Stafström, C. Ocal, B. Nieto-Ortega, J. Casado, J. T. López Navarrete, R. Lazzaroni, S. De Feyter, D. B. Amabilino, *J. Am. Chem. Soc.* **2010**, *132*, 9350–9362; b) F. García, L. Sánchez, *J. Am. Chem.Soc.* **2012**, *134*, 734–742.

[10] a) P. Jonkheijm, P. van der Schoot, A. P. H. J. Schenning, E. W. Meijer, *Science* **2006**, *313*, 80-83; b) M. M. J. Smulders, A. P. H. J. Schenning, E. W. Meijer, *J. Am. Chem. Soc.* **2008**, *130*, 606–611; c) U. Mayerhöffer, F. Würthner, *Chem. Sci.* **2012**, *3*, 1215–1220; d) J. M. Malicka, A. Sandeep, F. Monti, E. Bandini, M. Gazzano, C. Ranjith, V. K. Praveen, A. Ajayaghosh, N. Armaroli, *Chem. Eur. J.* **2013**, *19*, 12991–13001; e) C. Rest, R. Kandanelli, G. Fernández, *Chem. Soc. Rev.* **2015**, *44*, 2543–2572; f) A. Sandeep, V. K. Praveen, K. K. Kartha, V. Karunakaran, A. Ajayaghosh, *Chem. Sci.* **2016**, *7*, 4460–4467.

[11] a) S. Ogi, K. Sugiyasu, S. Manna, S. Samitsu, M. Takeuchi, *Nat. Chem.* **2014**, *6*, 188–195; b) S. Ogi, V. Stepanenko, J. Thein, F. Würthner, *J. Am. Chem. Soc.* **2016**, *138*, 670–678; d) A. Aliprandi, M. Mauro, L. De Cola, *Nat. Chem.* **2016**, *8*, 10–15; e) A. Sorrenti, J. Leira-Iglesias, A. J. Markvoort, T. F. A. De Greef, T. M. Hermans, *Chem. Soc. Rev.* **2017**, DOI: 10.1039/C7CS00121E.

[12] For solvent assisted depolymerization studies, see: a) P. A. Korevaar, C. Schaefer, T. F. De Greef, E. W. Meijer, *J. Am. Chem. Soc.* **2012**, *134*, 13482–13491; b) J. Buendía, L. Sánchez, *Org. Lett.* **2013**, *15*, 5746–5749; c) P. A. Korevaar, C. J. Newcomb, E. W. Meijer, S. I. Stupp, *J. Am. Chem. Soc.* **2014**, *136*, 8540–8543.

[13] a) K. Yoosaf, A. Llanes-Pallas, T. Marangoni, A. Belbakra, R. Marega, E. Botek, B. Champagne, D. Bonifazi, N. Armaroli, *Chem. Eur. J.* **2011**, *17*, 3262–3273; b) A. Gopal, R. Varghese, A. Ajayaghosh, *Chem. Asian J.* **2012**, *7*, 2061–2067.

10.1002/anie.201707392

COMMUNICATION

Insights on the evolution of chiral super-helix of π-systems through helicity reversal are reported. Concentration and temperature dependent decoiling and depolymerization experiments and morphological analysis reveal that the initial formation of the chiral elementary fibers are controlled by molecular chirality, whereas the hierarchical assembly of the chiral fibers to super-helical bundles goes to opposite direction.

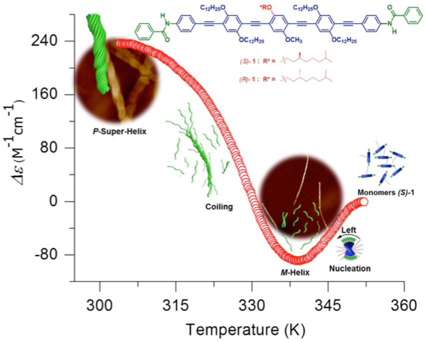

M. Hifsudheen, Dr. R. K. Mishra, Dr. B. Vedhanarayanan, Dr. V. K. Praveen, Prof. Dr. A. Ajayaghosh**

Page No. – Page No.

Helix to Super-Helix Transition in π-Systems Self-assembly: Superseding of Molecular Chirality at Hierarchical Level